Deciphering the CD73^{+} Regulatory γδ T Cell ecosystem associated with poor survival in Ovarian cancer

Ghita Chabab[1], Henri-Alexandre Michaud[1,2], Cécile Dejou[1], Laure-Agnès Chépeaux[1,2], Yaël Glasson[1,2], Florence Boissière[3], Marion Lenain[1], Anne-Sophie Dumé[1,2], Pauline Sarrant[1,2], Gabriel Chemin[4], Pauline Wajda[4], Bertrand Dubois[4], Anna MacManus[1,5], Pierre-Emmanuel Colombo[6], Michel Fabbro[7], Nathalie Bonnefoy[1#,] Maeva Chauvin[8#,] and Virginie Lafont[1#*]

[1] IRCM, Institut de Recherche en Cancérologie de Montpellier, INSERM U1194, Université de Montpellier, Institut régional du Cancer de Montpellier, 34298 Montpellier, France

[2] Plateforme de Cytométrie et d'Imagerie de Masse de Montpellier, Institut de Recherche en Cancérologie de Montpellier, INSERM U1194 - UM – ICM, Montpellier, France

[3] Translational Research Department, Institut Régional du Cancer Montpellier, 34298 Montpellier, France

[4] Cancer Immune Surveillance and Therapeutic Targeting Laboratory, Centre de Recherche en Cancérologie de Lyon (CRCL) INSERM U1052-CNRS UMR5286, Centre Léon Bérard, Université Claude Bernard Lyon 1, France

[5] Molecular Biosciences/Cancer Biology Program, Heidelberg University and German Cancer Research Center (DKFZ), Heidelberg, Germany

[6] Oncology Surgery Department, Institut régional du Cancer de Montpellier, 34298 Montpellier, France

[7] Medical oncology Department, Institut Régional du Cancer Montpellier, 34298 Montpellier, France

[8] Pediatric Surgical Research Laboratories, Massachusetts General Hospital, Boston, MA, USA - Department of Surgery, Harvard Medical School, Boston, MA, USA.

[#] Co-last authors

Running tiltle: Ecosystem and role of γδ T cells in human ovarian cancer

* Corresponding author: Dr Virginie Lafont, IRCM, INSERM U1194, 208 rue des Apothicaires, 34298 Montpellier cedex 5 France, Tel: +33.(0)4.11.28.31.47 email: virginie.lafont@inserm.fr

The authors declare no potential conflicts of interest.

Abstract

The ability of tumor cells to overcome immune surveillance is an essential step in tumor development and progression. Among the immune cells playing a role in tumor control, γδ T cells contribute to the immune response against many tumor types through their direct cytotoxic activity against cancer cells and their capacity to regulate the functions of other immune cells. However, their presence in the tumor microenvironment is also associated with poor prognosis, suggesting that γδ T cells may also have pro-tumor activities. We previously described a regulatory γδ T-cell subset that expresses CD73 and produces IL-10, IL-8 and adenosine. Here, we report a higher CD73+ γδ T cell density in the tumor microenvironment of ovarian cancer samples from patients with short-term than long-term survival. Starting from this original observation, we investigated their neighborhood and described a specific ecosystem according to their pro-tumor functions.

Introduction

Ovarian cancer is devastating due to its poor prognosis, with a 30% relative survival rate at 5 years, as it is usually diagnosed at an advanced stage (stage III/IV according to the FIGO system, which is a standardized system developed by the International Federation of Gynecology and Obstetrics) (1). Ovarian carcinoma accounts for over 90% of all ovarian cancer cases, and high-grade serous ovarian carcinoma (HGSOC) is the most prevalent and aggressive subtype, mainly due to resistance to platinum-based therapies (2,3). The mechanisms underlying recurrence, metastasis and resistance to therapy in ovarian cancer may be attributed partly to the tumor microenvironment (TME)which can suppress anti-tumor immunity by recruiting and promoting immune-suppressive cells, particularly from the immune compartment (4). In line with this, patients with HGSOC respond poorly to immune checkpoint inhibitors (5–7). The TME can affect, positively or negatively, solid tumor progression, including ovarian cancer (8). Indeed, the infiltration of various immune cell types into the TME is associated with the clinical outcome of patients with ovarian cancer. For example, tumor infiltration by CD3+ and CD8+ lymphocytes is associated with better survival in ovarian cancer (9,10), whereas the presence of infiltrating regulatory T cells (Tregs) predicts poor survival. Moreover, we previously showed that the density of γδ T cells is higher in ovarian tumor tissue than in normal matched ovarian tissue and tends to be higher in FIGO III/IV (i.e. advanced cancer) than low-stage tumors (11).

66 γδ T cells are unconventional T lymphocytes defined by the expression of a specific T cell
67 receptor (TCR) consisting of the Vγ and Vδ chains. In humans, there are two main γδ T-cell
68 subtypes, depending on the Vδ chain expressed: (i) Vδ2 T cells, mainly represented by the
69 innate Vγ9Vδ2 T-cell subset, that predominate in blood and recognize phosphorylated non-
70 peptide antigens, called phosphoantigens; and (ii) non-Vδ2 T cells, mainly represented by the
71 Vδ1 subset, that predominate in tissues and recognize stress-induced antigens (12–14). Both
72 subsets contribute to the immune response against cancer, particularly through their potent
73 effector functions allowing direct elimination of tumor cells and the recruitment of other
74 immune cells with anti-tumor activity (15). However, in addition to their anti-tumor functions,
75 γδ T cells have also been associated with pro-tumor functions in some cancer types.
76 Specifically, IL-17A-producing γδ T cells with pro-tumoral functions have been described in
77 murine breast, ovarian and hepatocellular cancer models and in human colorectal cancer (16–
78 18). In human breast cancer, γδ T cells have immunosuppressive functions associated with the
79 induction of dendritic cell senescence (19). Furthermore, in murine and human pancreatic
80 ductal adenocarcinoma, γδ T cells inhibit αβ T-cell activation and their infiltration via the PD-
81 L1/PD-1 pathway, thereby favoring tumor progression (20). Similarly, it has been reported that
82 in ovarian cancer, γδ T cells suppress the proliferation of CD4+ naive T cells (21). Altogether,
83 these data support the hypothesis that some γδ T-cell subsets may have immunosuppressive
84 functions and favor tumor progression in some solid tumor types. In agreement, we recently
85 identified in human blood samples a γδ T-cell subset, found in both Vδ2 and Vδ1 populations,
86 that expresses the ectonucleotidase CD73 and produces adenosine, an immunosuppressive
87 molecule (22,23). This cell subset also produces IL-10 and IL-8 and inhibits conventional T-cell
88 proliferation in a CD73/adenosine-dependent manner (22,23). Based on these findings, here,
89 we explored the potential regulatory role of CD73+ regulatory γδ T cells in the immune
90 landscape of ovarian cancer. Starting from our original observation that the presence of CD73+
91 γδ T cells is associated with poor clinical outcome in human ovarian cancer, we characterized
92 the profile and investigated the neighborhood of both CD73+ and CD73- γδ T cell populations
93 present in the ovarian TME and found a specific ecosystem according to their pro- and anti-
94 tumor functions.
95
96 **Materials and methods**

97 ***Tissue sample collection: Ovarian*** tissue samples were obtained from the Biological Resources
98 Center of Montpellier Cancer Institute (ICM, France), and were collected from patients with
99 HGSOC following the French regulations, under the supervision of the investigator Dr Fabbro.
100 The collection was declared to the French Ministry of Higher Education and Research
101 (declaration number DC-2008–695). The study was approved by the ICM Institutional Review
102 Board (ICM-CORT-2020-32). Clinical data (e.g., age, treatment, TNM, grade) were obtained by
103 reviewing the medical files. All samples were collected from biopsies taken at the time of
104 diagnosis, prior to any treatment. Nearly all tumors (95% of patients) exhibited TP53
105 mutations. Due to the lack of variability in TP53 status, no meaningful stratification was
106 performed based on this factor.
107
108 ***Ovarian cancer tumor microarray (TMA):*** TMAs regrouping 95 HGSOC samples were
109 constructed to retrospectively compare long-term (LT, >5 years) vs short-term (ST, <5 years)
110 ovarian cancer survivors. For each tumor sample, two cores (1 mm in diameter) were sampled
111 from different malignant areas. Of the 95 tumors sampled on TMA, 91 (48 LT and 43 ST) could
112 be analyzed, due to the absence of interpretable spots for 4 of them. The main
113 clinicopathological characteristics of this cohort are presented in Table S1.
114
115 ***Immunohistochemistry (IHC):*** 3 µm thin TMA sections were mounted on Flex microscope
116 slides (Agilent Technologies) and dried at room temperature (RT) overnight before IHC. The
117 PTLink system (Agilent Technologies) was used for de-paraffinization and heat-induced
118 antigen retrieval in High pH Buffer (Agilent Technologies) at 95°C for 15 min. IHC was
119 performed using the Dako Autostainer Link48 platform (Agilent Technologies).
120 Briefly, after endogenous peroxidase neutralization, TMA sections were incubated with the
121 mouse monoclonal anti-TCR δ antibody (Clone H-41, Santa Cruz Biotechnology) at RT for 30
122 min. This was followed by an amplification step with a mouse linker and the Flex Detection
123 System (Agilent Technologies) and 3,3'-diaminobenzidine as substrate. Sections were
124 counterstained with Flex Hematoxylin (Agilent Technologies). A NanoZoomer slide scanner
125 system (Hamamatsu Photonics) was used to digitalize the stained TMA sections with a ×40
126 objective. Immunoreactive cells were identified on the digitalized slides with the NDP.view2
127 software.

128 ***Immunofluorescence:*** After de-paraffinization, TMA sections underwent antigen retrieval
129 using 1X Target Retrieval Solution (S2367, Agilent Technologies). Then, they were incubated
130 in 1X Superblock Blocking Buffer (37515, Thermofisher) for 45 min followed by 1h incubation
131 in FcR Blocking solution (130-059-901, Miltenyi Biotech). After washing, TMA sections were
132 incubated with primary antibodies against γδ TCR (H-41, Santa Cruz, mouse, 1/25) and CD73
133 (D7AF9A, Cell Signaling Technology, rabbit, 1/100) at 4°C overnight and washed. Then,
134 sections were incubated with secondary goat anti-rabbit Alexa Fluor Plus 555 (A32732,
135 Thermofisher) and goat anti-mouse Alexa Fluor 647 (A21236, Thermofisher) antibodies.
136 Finally, sections were counterstained with DAPI and imaged with an AxioScan (Zeiss) to obtain
137 high-power field images. TMA sections were analyzed by two investigators blinded to the
138 clinicopathological characteristics and survival outcomes. Cell density was assessed by
139 counting the number of CD73- and CD73+ γδ T cells per spot (1 mm^2) and calculated as the
140 mean of two spots.
141
142 ***Survival analysis*****:** Categorical variables were presented as frequency distributions and
143 continuous variables as medians and ranges. Categorical variables were compared with the
144 Pearson's chi-square test. Overall survival (OS) was defined as the time between the date of
145 surgery and the date of death (whatever the cause). Patients lost to follow-up were censored
146 at the last documented visit. The Kaplan–Meier method was used to estimate the OS.
147 Differences in survival rates were compared using the log–rank test. Hazard ratios (HR) are
148 given with their 95% confidence interval (95% CI). Statistical analyses were performed with
149 STATA 16.0 (StatCorp, College Station, TX, USA).
150
151 ***Tumor dissociation:*** Freshly samples of resected ovarian tumors from patients with HGSOC
152 were cut into small pieces (~1 mm^3) and incubated in RPMI medium with a digestion solution
153 (1mg/mL collagenase IV from Sigma - C5138-100mg - and 0.2 mg/mL DNase I from Roche -
154 11284932001) at 37°C for 30 min, interspaced by two rounds of mechanical dissociation with
155 gentle flushing of the mixture. The obtained single-cell suspensions were filtered and stained
156 for immunophenotyping, or incubated at 37°C with Golgi stop for 1 h in complete medium
157 before performing immunostaining for cytokine analysis, as described in the next section.
158

159 ***Flow cytometry analysis:*** After dissociation, cells were washed in cold PBS and incubated with
160 a Fc receptor blocking reagent, to minimize non-specific binding of antibodies to Fc receptors
161 (130-059-901, Miltenyi Biotec), and a fluorescent cell viability marker (C36628, Beckman
162 Coulter) at 4°C for 15 min. Then, primary antibodies against surface markers were added in
163 PBS-2% fetal calf serum (FCS) at 4°C for 30 min. If no intracellular staining was performed, cells
164 were washed and fixed in 1% paraformaldehyde. If an intracellular staining was performed,
165 cells were washed and then fixed and permeabilized using the FOXP3 Fixation and
166 Permeabilization Kit (00-5523-00, eBioscience) at RT for 20 min, following the manufacturer's
167 protocol. Intracellular staining was performed by incubating cells with primary conjugated
168 antibodies diluted in intracellular blocking solution at 4°C for 1 h. Cells were washed and fixed
169 in 1% paraformaldehyde. The antibodies used for flow cytometry experiments are listed in
170 Table S2. Data were acquired with a Cytoflex LX cytometer (Beckman-Coulter) and analyzed
171 with the FlowJo software.
172
173 ***Cancer-associated fibroblast (CAF) isolation from tumor samples and immunofluorescence***
174 ***staining:*** After tumor sample dissociation and filtration, the fraction left in the filters was
175 collected and cultured in DMEM-F12 with 10% FCS until full adherence. The medium was
176 changed every 2 or 3 days and cells were passaged once they reached confluence.
177 Immunofluorescence staining with antibodies against alpha smooth muscle actin (α-SMA)
178 (F3777, Sigma, 1/200) and vimentin (C9080, Sigma, 1/600) was used to confirm the CAF
179 phenotype. After 15 days in culture and confirmation of their phenotype, CAFs were then used
180 for ELISA experiments, as described below. ***Ovarian cancer cell line culture:*** Cells were
181 cultured in DMEM-F12 with 10% FCS. Medium was changed every 2 or 3 days and cells were
182 passaged once they reached confluence. Cells were then used for ELISA experiments as
183 described below.
184
185 ***IL-6 ELISA:*** 1.10^5 cells were plated in 48-well plates in 0.5 mL of complete cell culture medium
186 (DMEM 10%SVF). After 24 h, supernatants were removed and 0.5 mL of fresh medium was
187 added. IL-6 production in the supernatants of primary human ovarian CAF cells and four
188 different human ovarian cancer cell lines (SKOV3, OVCAR3, OVCAR8, Kuramochi) was
189 evaluated 24 h after changing the medium using the Human IL-6 DuoSet ELISA Kit (DY206-05,
190 R&D Systems) following the manufacturer's instructions.

191

192 ***Imaging Mass Cytometry (IMC)-based tissue selection:*** Four ovarian tumors from the ST
193 survivor group were selected based on the γδ T-cell infiltration density. From whole formalin-
194 fixed paraffin-embedded tumor blocs, three sections were cut. One was stained with
195 hematoxylin-eosin-saffron to identify tissue structures; one was used for IHC to localize γδ
196 TCR, and one for IMC labeling and analysis. Based on the IHC data, 36 regions of interest (ROI)
197 were selected and analyzed by IMC.

198

199 ***IMC - tissue labeling:*** After de-paraffinization and antigen retrieval using the Dako Target
200 Retrieval Solution at pH 9 (S2368, Agilent Technologies) in a water bath (96°C for 30 min),
201 tissue sections were encircled with a Dako Pen, incubated with Superblock™ (37515,
202 Thermofisher Scientific) at RT for 45 min, and then with human FcR Blocking Reagent (130-
203 092-575, Miltenyi) at RT for 1 h. After three washes (8 min/each) in PBS/0.2% Triton X-100
204 (PBS-T), metal-tagged antibodies (list in Table S3) were diluted in PBS/1% BSA buffer. After
205 incubation with the primary antibodies at 4°C overnight, sections were washed in PBS-T three
206 times (8min/each) and nuclei were stained with iridium 191 and 193 (1:400 in PBS; Standard
207 Biotools), a DNA intercalator, at RT for 30 min. Sections were washed in PBS for 5 min, then in
208 distilled water for 5 min, and dried at RT for 30 min.

209

210 ***IMC - data acquisition:*** Images were acquired with the Hyperion Imaging System coupled to a
211 Helios time-of-flight mass cytometer (Standard Biotools) according to the manufacturer's
212 instructions. After selection, the ROIs were ablated with a UV laser at 200Hz. The Hyperion
213 Imaging System was calibrated to ensure system stability and reproducibility following the
214 manufacturer's instructions. Data were exported as MCD files and visualized using MCD™
215 viewer 1.0.560.6.

216

217 ***IMC – data processing and cell segmentation***: Tiff files were extracted from the raw data,
218 denoised and segmented using a custom pipeline based on the Steinbock framework with
219 Docker container (Deepcell)(24). Then, the segmentation masks were extracted based on the
220 iridium 191 and 193 nuclear staining and CD20, CD14, CD57, CD16, PanCK, CD3, CD66b, CD11c,
221 CD4, CD68, TCR γδ, CD8a, CD15, GrB, Ki67, HLA-DR and PDL1 staining (membrane/cytoplasm
222 markers). Default settings were kept for segmentation (pixel size at 1µm, whole-cell

223 segmentation, no normalization, and mean aggregation). The mean signal intensities for each
224 marker and for each cell were extracted from the .tiff files of each channel and the
225 segmentation masks with the *computeFeatures* function of the R package EBImage (25). Then,
226 data were exported in the fcs format with the R package flowCore (26).
227
228 ***Manual gating:*** Hierarchically gating and specific marker intensity were used to identify
229 immune cell subsets using FlowJo v10.10 (Supplementary Fig. 3A). Positivity thresholds were
230 checked by comparing the signal intensity of a marker with its intensity on the raw image using
231 an in-house application. Then, the gates were exported and reimported into R for further
232 analysis.
233
234 ***Single-cell clustering:*** Immune cell clustering was performed using the Rphenograph package
235 with k=50 and based on normalized channels. Clusters with similar marker expression profiles
236 were combined with cell types to account for over-clustering.***IMC – Generation of neighbors:***
237 Neighboring cells were extracted with a homemade R function. To identify its neighbors, each
238 cell was considered as the center of a circle. Then, the following formula derived from the
239 Pythagorean theorem was used:
240 $$\sqrt{|xC - xO|^2 + |yC - yO|^2} \leq R$$
241 where *xC* and *yC* are the coordinates of the cell centroid of interest, *xO* and *yO* the coordinates
242 of other cell centroids, and R the radius defined at 12µm. For each ROI, every cell for which
243 the equation was true was considered a neighboring cell and exported in fcs format. The radius
244 distance of 12µm was chosen to identify the cells that were most likely in contact with the cell
245 of interest.
246 ***Statistical analysis:*** The Mann-Whitney, log-rank, or Wilcoxon signed rank test was used to
247 analyze the results depending on the experiment (the used tests are mentioned in the figure
248 legends). A p value <0.05 was considered significant. Analyses were performed with GraphPad
249 Prism, version 8. *p<0.05; **p<0.01; ***p<0.001; ****p<0.0001
250

251 **Results**

252 ***CD73+ γδ tumor-infiltrating lymphocyte (TIL) density correlate with worse clinical outcomes***
253 ***in patients with ovarian cancer***

254 We and others showed that the density of γδ T cells is higher in ovarian cancer than in normal
255 ovarian tissue samples and that the number of γδ T cells is positively correlated with advanced
256 clinicopathological features of ovarian cancer (11). However, the potential role of γδ T cells in
257 ovarian cancer outcomes remains unclear. A study reported that in ovarian cancer, outcome
258 is positively influenced by the functionality of γδ T cells, measured by their ability to produce
259 Th1 cytokines, and negatively affected by the proportion of CD39+ T cells (27). Therefore, to
260 clarify their role, we analyzed the impact of γδ T-cell density on cancer progression in a cohort
261 of 91 patients with ovarian cancer (n=43 ST and n=48 LT survivors) for whom clinical data were
262 collected over the years. Regardless of whether patients received chemotherapy before or
263 after surgery, all analyzed samples were collected before treatment. Their median follow-up
264 was 13.44 years (95% CI [11.67-15.47]) and their median survival was 5.14 years (95% CI [3.75
265 - 6.08]). We first quantified by immunofluorescence staining all γδ T cells and then the CD73-
266 and CD73+ γδ T-cell subtypes. The densities of total (Fig. 1A), CD73+ (Fig. 1B) and CD73- (Fig.
267 1C) γδ T cells were significantly higher in ST survivors than in LT survivors, suggesting that the
268 presence of γδ T cells at the tumor site is associated with poor survival. We next investigated
269 the association between total, CD73+ and CD73- γδ T cells and OS in these 91 patients. Overall
270 survival (OS) was significantly longer in patients with low density of γδ T cells compared to
271 those with a high density ($p < 0.05$; median OS [IC50] low density = 6.099 years vs. high density
272 = 3.685 years; Fig. 1D). Similarly, OS was significantly shorter in patients with high density than
273 those with low density of CD73+ γδ T cells ($p < 0.001$; OS [IC50] low density = 6.077 years vs.
274 high density = 3.229 years; Fig. 1E) and this difference is even more pronounced than that
275 observed for total γδ T cells. The OS [IC50] of patients with high $CD73^+$ γδ T cell density was
276 even shorter than those with high total γδ T cell density (3.229 years vs 3.685 years),
277 suggesting a more detrimental role of $CD73^+$ γδ T cell subset. In contrast, $CD73^-$ γδ T cell
278 density did not significantly affect survival although OS was lower for high density (p = ns; OS
279 [IC50] low density = 6.099 years vs high density = 4.175 years; Fig. 1F). These reinforce the
280 hypothesis that although the density of γδ T cell subsets is higher in short-term (ST) survivors,
281 the effect γδ T cells on survival is mostly due to the CD73+ subset suggesting that the presence
282 and density of CD73+ γδ T cells may be a potential prognostic marker in ovarian cancer.

283 In parallel, the analysis of TCGA data revealed a strong association between a CD73+ tumor
284 microenvironment and poor patient outcomes (Fig. 2A). To investigate whether this CD73+
285 microenvironment correlates with γδ T cell infiltration, contributing to reduce survival as
286 demonstrated in Figure 1, we analyzed single-cell RNA sequencing (scRNA-seq) data from 20
287 untreated ovarian cancer samples. These samples were extracted from the GSE147082,
288 GSE241221, and GSE235931 datasets and pooled with Seurat's integration pipeline (28,29)
289 (Fig. 2B). Patients were divided into two groups based on median NT5E gene expression levels
290 (gene encoding CD73): CD73/NT5E-Low and CD73/NT5E-High (n=10 per group) (Fig. 2B).
291 Interestingly, expressions of specific γδ T cell transcripts such as TRDC (coding the TCRδ chain),
292 TRGC1 and TRGC2 (both coding TCRγ chain) are higher in TME overexpressing NT5E (CD73)
293 (Fig 2C). In addition, the following cytokine expression (CXCL8, IL-10, IL-6) (Fig. 2D) was higher
294 in the CD73/NT5E-High than CD73/NT5E-Low group as well as higher proportion of CAFs and
295 γδ T cells (Fig. 2E). These population enrichments suggest that the expression of IL-6, IL-10 and
296 CXCL8 and the density of γδ T cells and CAFs are significantly higher in CD73/NT5E-rich TMEs
297 than in CD73/NT5E-low TMEs. To validate these observations and to further explore these
298 relationships between cell subsets in different TMEs, we performed a spatial proteomic
299 analysis using an innovative high-plexed technology that allows detailed profiling of cell
300 phenotypes and the tumor ecosystem.
301
302 ***Cell composition of human ovarian tumors from short-term survivors***
303 First, we investigated the tissue composition of ovarian tumor samples of 4 patients from the
304 ST survivor group of our cohort by multiplexed IMC using a specific protocol described in
305 Supplementary Fig. 2. We selected 38 region of interests (ROIs) corresponding to
306 approximately 56 mm^2 based on the γδ T-cell density identified by IHC, on a serial section.
307 Using a 31-marker panel (Table S3) and a specific gating strategy to identify tumor, stromal
308 and immune cells (Supplementary Fig. 3A-B), we analyzed the cell composition of the selected
309 ROIs (Supplementary Fig. 3C-D). We identified 17 cell types and observed heterogeneity
310 among tumor samples and ROIs. Tumor cells, identified as E-cadherin+ and PanCK+ cells, were
311 the most important cell type in all samples (46% of all cells), followed by immune cells (27%
312 of all cells) and fibroblasts (vimentin+ cells; 15% of all cells) (Supplementary Fig. 3D-E).
313 Moreover, α-SMA+ cells were 8% of all cells and <1% of cells represented the vascular
314 compartment (Supplementary Fig. 3E). The remaining cells (<3.5%), classified as

315 “undetermined” (Supplementary Fig. 3E), corresponded to cells with a nucleus, but that could
316 not be identified using our panel. The characterization of the immune infiltrate
317 (Supplementary Fig. 3D and F) showed that lymphoid cells represented ~75% of the immune
318 infiltrate and most of them were T cells. In the myeloid compartment, monocyte-derived
319 dendritic cells were the most abundant subset (~13%).
320
321 ***Phenotypic analysis of CD73+ and CD73- γδ TILs***
322 Based on γδ TCR expression, we analyzed the γδ T-cell compartments by IMC (Fig. 3A). The
323 proportion of γδ T cells was quite homogenous in all ROIs. They represented ~3% of the
324 immune compartment (Fig. C and ~20% of all γδ TILs were CD73+ (Fig. 3D). Although the ROIs
325 analyzed by IMC were selected based on the presence of γδ T cells, the results were consistent
326 with the flow cytometry (FC) data obtained using fresh ovarian tumor samples (n=7) (Fig. 3B-
327 D).
328 Unsupervised analysis of total γδ T cells from the IMC data allowed identifying eight clusters
329 based on the expression of immune checkpoints and functional markers (Fig. 3E). The tSNE
330 plots of the CD73+ and CD73- γδ T-cell subsets were clearly different (Fig. 3F). Clusters 1, 5, 6
331 and 8 were more abundant in the CD73- γδ T-cell subset, whereas clusters 3 and 7 were more
332 abundant in the CD73+ γδ T-cell subset (Fig. 3F and Supplementary Fig. 4A). Cluster 3 was
333 characterized by strong expression of PD-L1 and to a lesser extent of LAG-3 and TIM-3 (Fig. 3E
334 and G) and cluster 7 by expression of PD-1, LAG-3, CD39 and Ki-67. Among the most abundant
335 clusters in the CD73- γδ T-cell subset, cluster 1 was characterized by high expression of the
336 functional marker HLA-DR and the immune checkpoints TIM-3, PD-L1; cluster 5 by expression
337 of the immune checkpoints PD-1, CD39, LAG-3, and cluster 6 by expression of HLA-DR and PD-
338 L1. Cluster 8 was not characterized by any of the analyzed markers (Fig. 3E-G). Clusters 2 and
339 4 were not specific to any subset. In parallel, we performed conventional flow cytometry
340 analysis of immune checkpoint marker expression in fresh ovarian tumor samples (n=7). We
341 confirmed the higher expression of PD-L1 in the CD73+ γδ T-cell subset. PD-L2 also was
342 expressed in this subset, whereas TIGIT was more strongly expressed in the CD73- γδ T-cell
343 subset (SupplementaryFig. 4B). This suggested that PD-L1 or PD-L2 when expressed may also
344 contribute to the immunosuppressive functions of CD73+ γδ T cells.
345 We previously showed that regulatory γδ T-cell subsets, derived from *in vitro* culture of blood
346 healthy donors, are characterized by CD73 expression and IL-8 and IL-10 production.

347 Therefore, we investigated by flow cytometry the expression IFN-γ, IL-10 and IL-8 by γδ T cells
348 isolated from fresh ovarian cancer samples in correlation with CD73 expression (Fig. 3H and
349 supplementary Fig. 4C). The frequency of IL-8+ and IL-10+ cells was significantly higher in the
350 CD73+ γδ than in the CD73- γδ T-cell subset (75% versus 10% for IL-8, 45% versus 5% for IL-
351 10). Moreover, 35% of CD73+ γδ T cells expressed both cytokines. Conversely, the percentage
352 of IFN-γ+ cells was significantly higher in the CD73- than CD73+ γδ T-cell subset (70% versus
353 30%). Altogether, these results demonstrated that CD73+ γδ T cells from ovarian tumors have
354 a profile similar to that of the previously described regulatory CD73+ γδ T-cell subset (22,23)
355 and suggested that their immunosuppressive properties may be involved in the poorer clinical
356 outcome.
357
358 ***CD73+ and CD73- γδ TILs have phenotypically and functionally different ecosystems***
359 Besides the immune cell composition, the spatial location and interactions of immune cells
360 within the TME are essential for their functions and the effect on tumor development and
361 response to treatment.
362 Here, we investigated the γδ T-cell ecosystem by comparing the effector (CD73-) and
363 regulatory (CD73+) γδ T-cell neighborhoods and interactions by IMC. After identification and
364 localization of CD73+ and CD73- γδ T cells in ovarian cancer tissue sections (Fig. 4A), we
365 measured and compared the individual interactions between CD73+ and CD73- γδ T cells with
366 the other identified cell types. For both cell subtypes, we observed an heterogenous
367 environment but with significant differences. CD73- γδ T cells had a neighborhood significantly
368 enriched in tumor cells (24.4% versus 12.7% for CD73+ γδ T cells) (Fig. 4B and Supplementary
369 Fig. 5). Conversely, fibroblasts and CD4+ T cells tended to be more frequently in contact with
370 CD73+ than CD73- γδ T cells (Fig. 4B and C and Supplementary Fig. 5), suggesting that the
371 CD73+ γδ T-cell neighborhood is enriched in fibroblasts and CD4+ T cells. Comparison of the
372 CD73+ γδ T-cell ecosystem with the conventional regulatory T-cell (CD3+CD4+FOXP3+)
373 ecosystem revealed a specific CD73+ γδ T cell ecosystem (Supplementary Data Fig6).
374 We then determined the number of cells for all identified populations and chose to perform
375 a functional analysis only of the cell compartments containing more than 750 cells to obtain
376 robust results (Supplementary Fig. 7): tumor cells, fibroblasts, CD4+ and CD8+ T cells.
377 Unsupervised clustering of the tumor cell compartment allowed identifying eight cell
378 populations that were differentially abundant depending on whether they were in the vicinity

379 of effector (CD73-) or regulatory (CD73+) γδ T cells (Fig. 5A and Supplementary Fig. 8A).
380 Indeed, tumor cells expressed CD73 and the epithelial-to-mesenchymal transition (EMT)
381 marker ZEB-1, in the neighborhood of CD73+ γδ T suggesting migratory capacity (Fig. 5A).
382 Tumor cells in contact with CD73- γδ T cells expressed PD-L1. Altogether, these data suggest
383 that tumor cells in contact with CD73+ γδ T cells have a more aggressive phenotype. Similarly,
384 cluster analysis showed that fibroblasts in contact with CD73+ γδ T cells expressed CD73 and
385 PD-L1, whereas those in contact with CD73- γδ T cells expressed more CD39 and Ki-67 (Fig. 5B
386 and Supplementary Fig 8B).
387 Like for other cell types, unsupervised analysis of the T-cell compartment gave different tSNE
388 clustering plots in the neighborhood of CD73+ and CD73- γδ T cells for the CD4+ and CD8+ T
389 cell populations (Fig. 6A-B and Supplementary Fig. 8C-D). The cluster analysis revealed that
390 CD4+ T cells in contact with effector γδ T cells (i.e. the CD73- subset) express HLA-DR and/or
391 PD-1, both activation markers. In contrast, cells that interacted with CD73+ γδ T cells displayed
392 expression of CD73, PD-1, CD39, and LAG-3, which may indicative of an exhausted phenotype
393 (Fig. 6A). For CD8+ T cells, the CD73+ and PD-1+ cluster was much more abundant in the
394 neighborhood of CD73+ γδ T cells (Supplementary Fig 8D).
395 Although the density of fibroblasts and T cells surrounding CD73- and CD73+ γδ T cells was
396 similar, the functional phenotype of these cell populations differed, resulting in distinct
397 ecosystems, suggesting that CD73+ γδ T cells are located in an immunosuppressive niche in
398 close contact with tumor cells. Comparison of CD73+ γδ T cells and Treg revealed specific
399 neighborhoods for each population (Supplementary Fig. 6), suggesting that the mechanisms
400 responsible for establishing an immunosuppressive microenvironment are specific to CD73+
401 regulatory γδ T cells.
402
403 ***Impact of IL-6 produced by ovarian CAFs and tumor cells on γδ T cells***
404 We and others provided evidence that soluble factors, such as cytokines, can modulate the
405 functions of γδ T cells (30). Specifically, we showed that IL-21 promotes the development of a
406 pro-tumoral γδ T-cell subset, characterized by CD73 expression and production of
407 immunosuppressive molecules, such as adenosine, IL-10 and IL-8 (22) . Others have shown
408 that CAFs from breast tumors produce IL-6 and induce the differentiation of CD73+ γδ T cells
409 from normal breast tissue into immunosuppressive T cells (31). As IL-6 is strongly expressed
410 in the ovarian TME (32), we hypothesized that CAF-produced IL-6 may be involved in the

411 development or differentiation of CD73+ γδ T cells in ovarian cancer. We isolated CAFs from
412 freshly resected ovarian tumor samples (n=3) and confirmed their phenotype/purity by α-SMA
413 and vimentin staining (Fig. 7A). We then measured IL-6 in their supernatants and in the
414 supernatants of four ovarian tumor cell lines by ELISA. Both CAFs and ovarian tumor cell lines
415 produced IL-6, but the amounts were much higher in CAF supernatants than in tumor cells
416 (1500 pg/mL vs ~70pg/mL) (Fig. 7B). Additionally, as reported by other teams and by our group
417 (11,22,31), we confirmed that IL-6, similar to IL-21, promotes the development of the CD73+
418 γδ T cell subset from blood-derived γδ T cells of healthy donors. (Fig. 7C and D). Altogether,
419 these data suggest that the cross-talk between CAFs and γδ T cells in the TME through IL-6
420 production may favor an immunosuppressive niche that promotes tumor growth and immune
421 escape.
422
423 **Discussion**
424 Investigating the presence, functions and location of immune cells in the TME is essential for
425 developing effective immunotherapy strategies. In this study, we report the presence of
426 CD73+ γδ T cells, a regulatory γδ T-cell subset with immunosuppressive functions, in the
427 ovarian TME of HGSOC and show that their density is associated with poorer clinical outcome
428 in these patients (Fig 1). Although γδ T cells have often been associated with good cancer
429 prognosis (33), several reports in ovarian cancer have provided evidence of their negative
430 impact. For instance, γδ T cells have been positively associated with advanced
431 clinicopathological features of ovarian cancer (34). Moreover, the presence of Vδ1+ cells
432 correlates with progression-free and OS in patients with triple-negative breast cancer (35).
433 Conversely, CD73+ γδ T cell infiltration has been correlated with worse clinical outcome in
434 patients with breast cancer (31). In line with our findings in ovarian cancer, the CD73+ γδ T-
435 cell subset appears to be involved in poor outcome in some cancer types, but the involved
436 mechanisms remain to be elucidated.
437 By combining scRNA-seq, high-plex IMC and *ex vivo* flow cytometry analysis of freshly resected
438 ovarian tumors, we described in detail the phenotype and ecosystem of CD73+ and CD73- γδ
439 T cells. CD73+ γδ T cells produce IL-10 and IL-8 and also express the immune checkpoints PD-
440 L1 and PD-L2, cytokines and ligands that may explain their regulatory functions and may be
441 involved in the immunosuppressive or pro-tumor mechanisms leading to tumor progression.
442 Indeed, IL-10 impairs the functions of effector cells, such as T and natural killer cells, while PD-

443 L1 and PD-L2 contribute to tumor immune evasion by binding to PD-1 and impair the function
444 of all PD-1+ effector immune cells. IL-8, also known as CXCL8, was originally classified as a
445 chemoattractant for neutrophils and myeloid-derived suppressor cells. It is now known to play
446 other important biological activities in various solid cancer types, such as induction/regulation
447 of angiogenesis and promotion of cancer cell growth, survival and migration (36,37). Several
448 studies have shown that IL-8 induces EMT in ovarian cancer cells and favors migration,
449 invasion and metastasis formation (38–40). IL-8 also promotes ovarian cancer growth in 3D
450 spheroid models (41). Moreover, CAF-derived IL-8 promotes the stemness and malignant
451 proliferation of ovarian cancer cells through NOTCH-3 signaling pathways (42). Conversely,
452 CD73- γδ T cells produce IFN-γ, express the PD-1 and TIGIT checkpoint molecules, and also
453 HLA-DR. Several studies have shown that human γδ T cells can express MHC class II molecules
454 and acquire professional antigen-presenting cell characteristics. Thus, ovarian CD73- γδ TILS
455 have effector T cell properties, whereas CD73+ γδ TILS have regulatory T cell properties.
456 We also performed a spatial analysis of the CD73+ and CD73- γδ T cell ecosystems in ovarian
457 cancer samples. We found that CD73+ γδ T cells were in close contact with tumor cells
458 expressing more mesenchymal markers, such as ZEB-1, a transcription factor associated with
459 EMT. This is consistent with CD73+ γδ T cell ability to produce IL-8, which has been described
460 as an inducer of several transcription factors involved in EMT and tumor cell migration, such
461 as ZEB-1 and snail (43). In addition, tumor cells close to CD73+ γδ T cells also expressed CD73,
462 which is involved in the generation of the immunosuppressive molecule adenosine from AMP
463 present in the TME. Conversely, tumor cells adjacent to CD73- γδ TILs expressed the immune
464 checkpoint PD-L1 that can be induced by IFN-γ, a cytokine largely produced by CD73- γδ T cells
465 ((44) and our experiments). The spatial analysis also revealed that fibroblasts/CAFs in contact
466 with CD73+ γδ T cells are functionally distinct from those in contact with the CD73- subset.
467 Specifically, one of the CAF clusters in contact with the CD73+ γδ T-cell subset expressed CD73.
468 Several studies have described CD73+ CAF subsets as tumor-promoting or
469 immunosuppressive CAFs. Using a 41-plex antibody panel designed to discriminate the
470 different CAF phenotypes by mass cytometry, Bodenmiller's group identified a subset, which
471 they termed tumor-like CAFs (tCAFs), with tumor-promoting and immunosuppressive effects
472 and characterized by CD73 and CD10 expression (45). Another study using a mouse model of
473 soft tissue sarcoma identified a CAF subset with a glycolytic signature and characterized by
474 CD73 expression. These glycolytic CAFs rely on GLUT-1-dependent expression of CXCL16 to

475 prevent cytotoxic T-cell infiltration into the tumor. Therefore, CD73+ CAFs could be considered
476 as immunosuppressive or pro-tumor CAFs. In the T-cell compartment, the spatial analysis
477 revealed a cluster of $CD4^+$ T cells expressing HLA-DR and/or PD-1 in proximity to the $CD73^-$ γδ
478 T-cell subset, suggesting a population with features consistent with recent activation or
479 immune engagement. Conversely, those in contact with CD73+ γδ T cells expressed CD73, PD-
480 1, CD39 and LAG-3, suggesting an exhausted phenotype. The spatial analysis of CD8+ T cells
481 highlighted a different clustering between cells in contact with CD73- and CD73+ γδ T cells,
482 particularly concerning the expression of immune checkpoint factors. Indeed, those in contact
483 with CD73+ γδ T cells expressed PD-1 and CD39, whereas those contact with CD73+ γδ T cells
484 expressed CD73 and Lag-3.
485 Cytokines can promote or inhibit tumor cell differentiation and immune cell
486 differentiation/functions and angiogenesis, and ultimately affect the patients' response to
487 therapy (8). Ovarian tumors are characterized by abnormal expression of many cytokines, such
488 as IL-6, IL-8 and IL-10, that affects all TME components and also patient survival (29). IL-8 and
489 IL-10 are produced by CD73+ γδ T cells and IL-6 by cells in their close environment. In addition,
490 γδ T-cell subsets can also produce cytokines with immunosuppressive properties, such as IL-
491 17A and TGF-β and can be involved in the immunosuppressive mechanisms of γδ T cells
492 and/or in their effect on tumor growth, as demonstrated in human colorectal cancer (18).
493 However, in the present study, ovarian cancer CD73+ γδ T cell subsets did not produce these
494 two cytokines (data not shown).
495 Studies in other cancer types demonstrated the existence of immunosuppressive or pro-
496 tumor γδ T-cell subsets. Daley et al showed in a murine pancreatic cancer model that tumor-
497 infiltrating γδ T cells have potent immunosuppressive functions through the PD-1/PD-L1 axis
498 (20). Specifically, 50% of infiltrating γδ T cells express PD-L1 and induce αβ T-cell exhaustion
499 through this mechanism. In our study, regulatory γδ T cells were characterized by the
500 expression of CD73 and of various immune checkpoint factors, such as PD-L1. These findings
501 suggest that, beyond the immunosuppressive effects mediated by IL-10 and IL-8, $CD73^+$ γδ T
502 cells may further promote immunosuppression and tumor progression via immune checkpoint
503 factor expression and adenosine production. In colorectal cancer, Lynch's group described a
504 γδ T-cell subset that expresses NKp80, produces AREG and induces tumor cell proliferation
505 (46). The existence of pro-tumor and immunosuppressive γδ T-cell subsets is now well

506 established and their role in some cancer types has been demonstrated; however, they
507 represent a heterogeneous population with different mechanisms.
508 Chronic inflammation is a cancer hallmark and is involved in tumor development and
509 progression. Inflammatory cytokines mediate chronic inflammation and are involved in cancer
510 progression by regulating, for example, immune cell functions. IL-6, which is present at high
511 levels in the ovarian TME, is associated with poor prognosis and increased tumor progression.
512 We and others reported that in ovarian tumors, IL-6 is mainly produced by CAFs and induces
513 CD73 expression by γδ T cells (Fig. 7 and 31). Thus, the proximity between CD73+ γδ T cells
514 and CAFs, observed by IMC, suggests crosstalk mechanisms whereby CAF-produced IL-6 would
515 lead to the recruitment or polarization of γδ T cells into regulatory CD73+ γδ T cells. By a
516 positive feedback, adenosine produced by CD73+ cells would increase IL-6 production in the
517 ovarian TME (Fig. 8). These findings are consistent with the work by Hu et al, who showed that
518 in human breast cancer, CAF-derived IL-6 induces γδ T-cell differentiation into the regulatory
519 CD73+ subset which produces high levels of adenosine following the activation of the IL-6/IL6-
520 R/STAT3 signaling pathway (31). They also showed that CD73+ γδ T cells could in turn promote
521 IL-6 secretion by CAFs through activation of the adenosine/A2BR/p38 MAPK pathway, thereby
522 forming a positive feedback loop (31). This interplay between CAFs and CD73+ γδ T cells could
523 be a general mechanism in solid tumors. The role of IL-8 in EMT and tumor cell migration cells
524 could also be included in this regulation loop, as shown in Figure 8. Consistently, our
525 transcriptomic analysis of ovarian tumors revealed that high expression levels of CD73 were
526 associated with increased expression of TRDC, IL6, IL10, and IL8, further supporting the
527 existence of this immunoregulatory and pro-tumoral network in the TME (Fig 2). Preliminary
528 data also indicate the presence of $CD73^+$ γδ T cells in pancreatic and colorectal cancers (data
529 not shown), however, their associated cellular ecosystem remains to be investigated. Overall,
530 our data provide a better understanding of the role of regulatory γδ T cells in the tumor
531 microenvironment and allow to propose mechanisms involving γδ T cells in the creation of a
532 specific immunosuppressive environment (Fig. 8), which could be a more general and existing
533 mechanism in solid tumors with a poor evolution.
534

535 **Acknowledgements**

536 This work was supported by the Institute National de la Santé et de la Recherche Médicale
537 (INSERM); Université Montpellier; the Institut Régional du Cancer de Montpellier (ICM), the

538 SIRIC Montpellier Cancer (Grant INCa_Inserm_DGOS_12553), the Fondation ARC and the
539 Ligue contre le Cancer. Ghita Chabab is supported by a Ph. D. studentship from the Fondation
540 pour la Recherche Médicale and Fondation ARC. We acknowledge the Clinical Resources
541 Center of the Montpellier Cancer Institute (CRB-ICM, n°BB-033-00059). We acknowledge the
542 imaging facility MRI, member of the national infrastructure France-BioImaging infrastructure
543 supported by the French National Research Agency (ANR-10-INBS-04, Investments for the
544 future).

545

546

547

548 **References**

549 1. Sung H, Ferlay J, Siegel RL, Laversanne M, Soerjomataram I, Jemal A, et al. Global Cancer
550 Statistics 2020: GLOBOCAN Estimates of Incidence and Mortality Worldwide for 36
551 Cancers in 185 Countries. CA: A Cancer Journal for Clinicians. 2021;71:209–49.

552 2. Hinchcliff E, Westin SN, Herzog TJ. State of the science: Contemporary front-line
553 treatment of advanced ovarian cancer. Gynecologic Oncology. Elsevier; 2022;166:18–24.

554 3. Luvero D, Milani A, Ledermann JA. Treatment options in recurrent ovarian cancer: latest
555 evidence and clinical potential. Ther Adv Med Oncol. SAGE Publications Ltd STM;
556 2014;6:229–39.

557 4. Drakes ML, Stiff PJ. Regulation of Ovarian Cancer Prognosis by Immune Cells in the Tumor
558 Microenvironment. Cancers (Basel). 2018;10:302.

559 5. Hamanishi J, Mandai M, Iwasaki M, Okazaki T, Tanaka Y, Yamaguchi K, et al. Programmed
560 cell death 1 ligand 1 and tumor-infiltrating CD8+ T lymphocytes are prognostic factors of
561 human ovarian cancer. Proc Natl Acad Sci U S A. 2007;104:3360–5.

562 6. Disis ML, Taylor MH, Kelly K, Beck JT, Gordon M, Moore KM, et al. Efficacy and Safety of
563 Avelumab for Patients With Recurrent or Refractory Ovarian Cancer: Phase 1b Results
564 From the JAVELIN Solid Tumor Trial. JAMA Oncol. 2019;5:393–401.

565 7. Ray-Coquard IL, Savoye A-M, Schiffler C, Mouret-Reynier M-A, Derbel O, Kalbacher E, et
566 al. Neoadjuvant and adjuvant pembrolizumab in advanced high-grade serous carcinoma:
567 the randomized phase II NeoPembrOV clinical trial. Nat Commun. Nature Publishing
568 Group; 2024;15:5931.

569 8. Baci D, Bosi A, Gallazzi M, Rizzi M, Noonan DM, Poggi A, et al. The Ovarian Cancer Tumor
570 Immune Microenvironment (TIME) as Target for Therapy: A Focus on Innate Immunity
571 Cells as Therapeutic Effectors. Int J Mol Sci. 2020;21:3125.

572 9. Ovarian Tumor Tissue Analysis (OTTA) Consortium, Goode EL, Block MS, Kalli KR, Vierkant
573 RA, Chen W, et al. Dose-Response Association of CD8+ Tumor-Infiltrating Lymphocytes
574 and Survival Time in High-Grade Serous Ovarian Cancer. JAMA Oncol. 2017;3:e173290.

575 10. Zhang L, Conejo-Garcia JR, Katsaros D, Gimotty PA, Massobrio M, Regnani G, et al.
576 Intratumoral T cells, recurrence, and survival in epithelial ovarian cancer. N Engl J Med.
577 2003;348:203–13.

578 11. Chabab G, Boissière-Michot F, Mollevi C, Ramos J, Lopez-Crapez E, Colombo P-E, et al.
579 Diversity of Tumor-Infiltrating, γδ T-Cell Abundance in Solid Cancers. Cells. 2020;9:1537.

580 12. Kabelitz D. γδ T-cells: cross-talk between innate and adaptive immunity. Cell Mol Life Sci.
581 2011;68:2331–3.

582 13. Vantourout P, Hayday A. Six-of-the-best: unique contributions of γδ T cells to
583 immunology. Nat Rev Immunol. 2013;13:88–100.

584 14. Adams EJ, Gu S, Luoma AM. Human gamma delta T cells: Evolution and ligand
585 recognition. Cell Immunol. 2015;296:31–40.

586 15. Kabelitz D, Serrano R, Kouakanou L, Peters C, Kalyan S. Cancer immunotherapy with γδ T
587 cells: many paths ahead of us. Cell Mol Immunol. 2020;17:925–39.

588 16. Coffelt SB, Kersten K, Doornebal CW, Weiden J, Vrijland K, Hau C-S, et al. IL-17-producing
589 γδ T cells and neutrophils conspire to promote breast cancer metastasis. Nature.
590 2015;522:345–8.

591 17. Ma S, Cheng Q, Cai Y, Gong H, Wu Y, Yu X, et al. IL-17A produced by γδ T cells promotes
592 tumor growth in hepatocellular carcinoma. Cancer Res. 2014;74:1969–82.

593 18. Wu P, Wu D, Ni C, Ye J, Chen W, Hu G, et al. γδT17 cells promote the accumulation and
594 expansion of myeloid-derived suppressor cells in human colorectal cancer. Immunity.
595 2014;40:785–800.

596 19. Peng G, Wang HY, Peng W, Kiniwa Y, Seo KH, Wang R-F. Tumor-infiltrating gammadelta
597 T cells suppress T and dendritic cell function via mechanisms controlled by a unique toll-
598 like receptor signaling pathway. Immunity. 2007;27:334–48.

599 20. Daley D, Zambirinis CP, Seifert L, Akkad N, Mohan N, Werba G, et al. γδ T Cells Support
600 Pancreatic Oncogenesis by Restraining αβ T Cell Activation. Cell. 2016;166:1485-
601 1499.e15.

602 21. Chen X, Shang W, Xu R, Wu M, Zhang X, Huang P, et al. Distribution and functions of γδ T
603 cells infiltrated in the ovarian cancer microenvironment. J Transl Med. 2019;17:144.

604 22. Barjon C, Michaud H-A, Fages A, Dejou C, Zampieri A, They L, et al. IL-21 promotes the
605 development of a CD73-positive Vγ9Vδ2 T cell regulatory population. Oncoimmunology.
606 2017;7:e1379642.

607 23. Chabab G, Barjon C, Abdellaoui N, Salvador-Prince L, Dejou C, Michaud H-A, et al.
608 Identification of a regulatory Vδ1 gamma delta T cell subpopulation expressing CD73 in
609 human breast cancer. J Leukoc Biol. 2020;107:1057–67.

610 24. Windhager J, Zanotelli VRT, Schulz D, Meyer L, Daniel M, Bodenmiller B, et al. An end-to-
611 end workflow for multiplexed image processing and analysis. Nat Protoc. 2023;18:3565–
612 613.

613 25. Pau G, Fuchs F, Sklyar O, Boutros M, Huber W. EBImage--an R package for image
614 processing with applications to cellular phenotypes. Bioinformatics. 2010;26:979–81.

615 26. Hahne F, LeMeur N, Brinkman RR, Ellis B, Haaland P, Sarkar D, et al. flowCore: a
616 Bioconductor package for high throughput flow cytometry. BMC Bioinformatics.
617 2009;10:106.

618 27. Foord E, Arruda LCM, Gaballa A, Klynning C, Uhlin M. Characterization of ascites- and
619 tumor-infiltrating γδ T cells reveals distinct repertoires and a beneficial role in ovarian
620 cancer. Sci Transl Med. 2021;13:eabb0192.

621 28. Kang H, Hwang S, Kang H, Jo A, Lee JM, Choi JK, et al. Altered tumor signature and T-cell
622 profile after chemotherapy reveal new therapeutic opportunities in high-grade serous
623 ovarian carcinoma. Cancer Sci. 2024;115:989–1000.

624 29. Olalekan S, Xie B, Back R, Eckart H, Basu A. Characterizing the tumor microenvironment
625 of metastatic ovarian cancer by single-cell transcriptomics. Cell Rep. 2021;35:109165.

626 30. Zhao Y, Niu C, Cui J. Gamma-delta (γδ) T cells: friend or foe in cancer development?
627 Journal of Translational Medicine. 2018;16:3.

628 31. Hu G, Cheng P, Pan J, Wang S, Ding Q, Jiang Z, et al. An IL6-Adenosine Positive Feedback
629 Loop between CD73+ γδTregs and CAFs Promotes Tumor Progression in Human Breast
630 Cancer. Cancer Immunol Res. 2020;8:1273–86.

631 32. Browning L, Patel MR, Horvath EB, Tawara K, Jorcyk CL. <no title>. Dove Medical Press;
632 2018;

633 33. Gentles AJ, Newman AM, Liu CL, Bratman SV, Feng W, Kim D, et al. The prognostic
634 landscape of genes and infiltrating immune cells across human cancers. Nat Med.
635 2015;21:938–45.

636 34. Foord E, Arruda LCM, Gaballa A, Klynning C, Uhlin M. Characterization of ascites- and
637 tumor-infiltrating γδ T cells reveals distinct repertoires and a beneficial role in ovarian
638 cancer. Sci Transl Med. 2021;13:eabb0192.

639 35. Wu Y, Kyle-Cezar F, Woolf RT, Naceur-Lombardelli C, Owen J, Biswas D, et al. An innate-
640 like Vδ1+ γδ T cell compartment in the human breast is associated with remission in
641 triple-negative breast cancer. Sci Transl Med. 2019;11:eaax9364.

642 36. Yuan A, Chen JJW, Yao P-L, Yang P-C. The role of interleukin-8 in cancer cells and
643 microenvironment interaction. Front Biosci. 2005;10:853–65.

644 37. De Larco JE, Wuertz BR, Rosner KA, Erickson SA, Gamache DE, Manivel JC, et al. A
645 potential role for interleukin-8 in the metastatic phenotype of breast carcinoma cells. Am
646 J Pathol. 2001;158:639–46.

647 38. Wen J, Zhao Z, Huang L, Wang L, Miao Y, Wu J. IL-8 promotes cell migration through
648 regulating EMT by activating the Wnt/β-catenin pathway in ovarian cancer. J Cell Mol
649 Med. 2020;24:1588–98.

650 39. Interleukin-8 promotes human ovarian cancer cell migration by epithelial-mesenchymal
651 transition induction in vitro - PubMed [Internet]. [cited 2024 Nov 20]. Available from:
652 https://pubmed-ncbi-nlm-nih-gov.proxy.insermbiblio.inist.fr/25373532/

653 40. Li Y, Liu L, Yin Z, Xu H, Li S, Tao W, et al. Effect of targeted silencing of IL-8 on in vitro
654 migration and invasion of SKOV3 ovarian cancer cells. Oncol Lett. 2017;13:567–72.

655 41. Uddin MM, Gaire B, Vancurova I. Interleukin-8 Induces Proliferation of Ovarian Cancer
656 Cells in 3D Spheroids. Methods Mol Biol. 2020;2108:117–24.

657 42. Ji Z, Tian W, Gao W, Zang R, Wang H, Yang G. Cancer-Associated Fibroblast-Derived
658 Interleukin-8 Promotes Ovarian Cancer Cell Stemness and Malignancy Through the
659 Notch3-Mediated Signaling. Front Cell Dev Biol. 2021;9:684505.

660 43. Zhao Z, Wang S, Lin Y, Miao Y, Zeng Y, Nie Y, et al. Epithelial-mesenchymal transition in
661 cancer: Role of the IL-8/IL-8R axis (Review). Oncology Letters. Spandidos Publications;
662 2017;13:4577–84.

663 44. Abiko K, Matsumura N, Hamanishi J, Horikawa N, Murakami R, Yamaguchi K, et al. IFN-γ
664 from lymphocytes induces PD-L1 expression and promotes progression of ovarian
665 cancer. Br J Cancer. Nature Publishing Group; 2015;112:1501–9.

666 45. Cords L, Tietscher S, Anzeneder T, Langwieder C, Rees M, de Souza N, et al. Cancer-
667 associated fibroblast classification in single-cell and spatial proteomics data. Nat
668 Commun. 2023;14:4294.

669 46. Harmon C, Zaborowski A, Moore H, St Louis P, Slattery K, Duquette D, et al. γδ T cell
670 dichotomy with opposing cytotoxic and wound healing functions in human solid tumors.
671 Nat Cancer. 2023;4:1122–37.

672

673

674

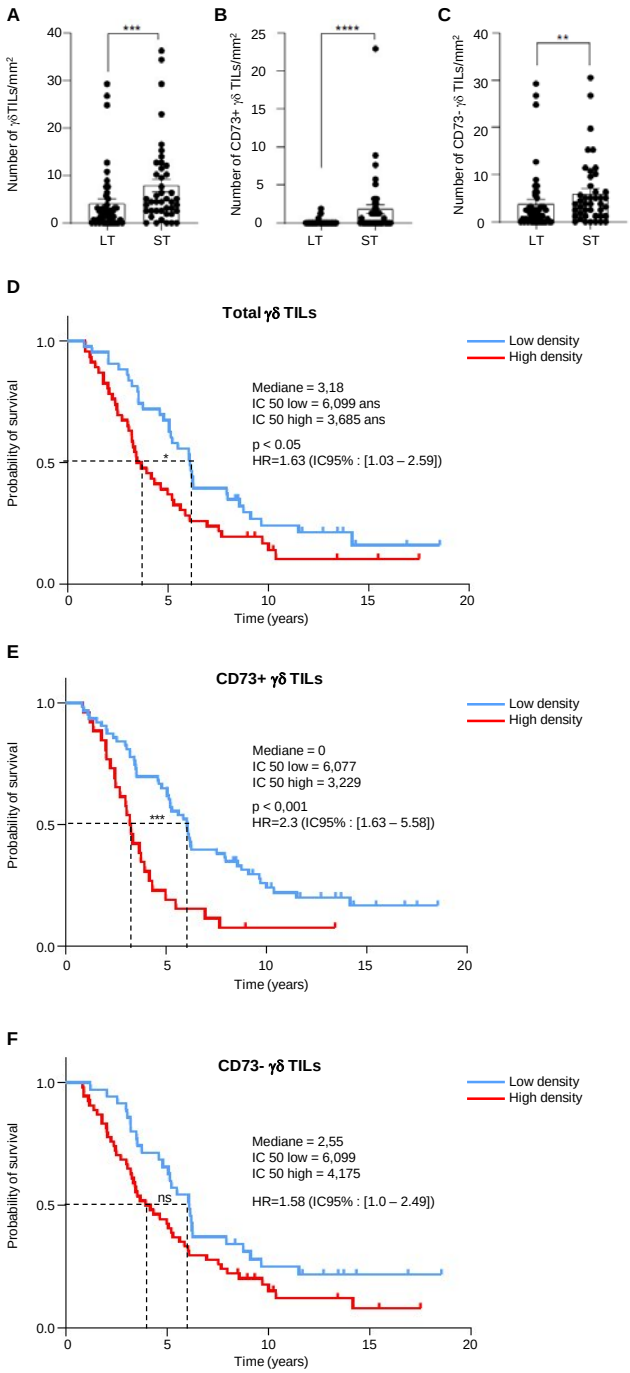

Figure 1. Relationship between γδ T cell infiltration and survival outcomes in ovarian cancer patients or correlation between γδ T cell infiltration and survival in patients with ovarian cancer

Scatter plots comparing the density of total γδ T cells (A), CD73+ γδ T cells (B), and CD73- γδ T cells (C) in short-term (ST, n=43) and long-term (LT, n=48) survivors. Overall survival analysis according to the density of total γδ T cells (D), CD73+ γδ T cells (E), and CD73- γδ T cells (F) in the same patients with ovarian cancer. Data are the mean ± SEM. ns: not significant; **p < 0.01; ***p < 0.001; ****p < 0.0001 (Mann-Whitney test for panels A, B and C; log-rank test for the survival analysis). TILs, tumor-infiltrating lymphocytes.

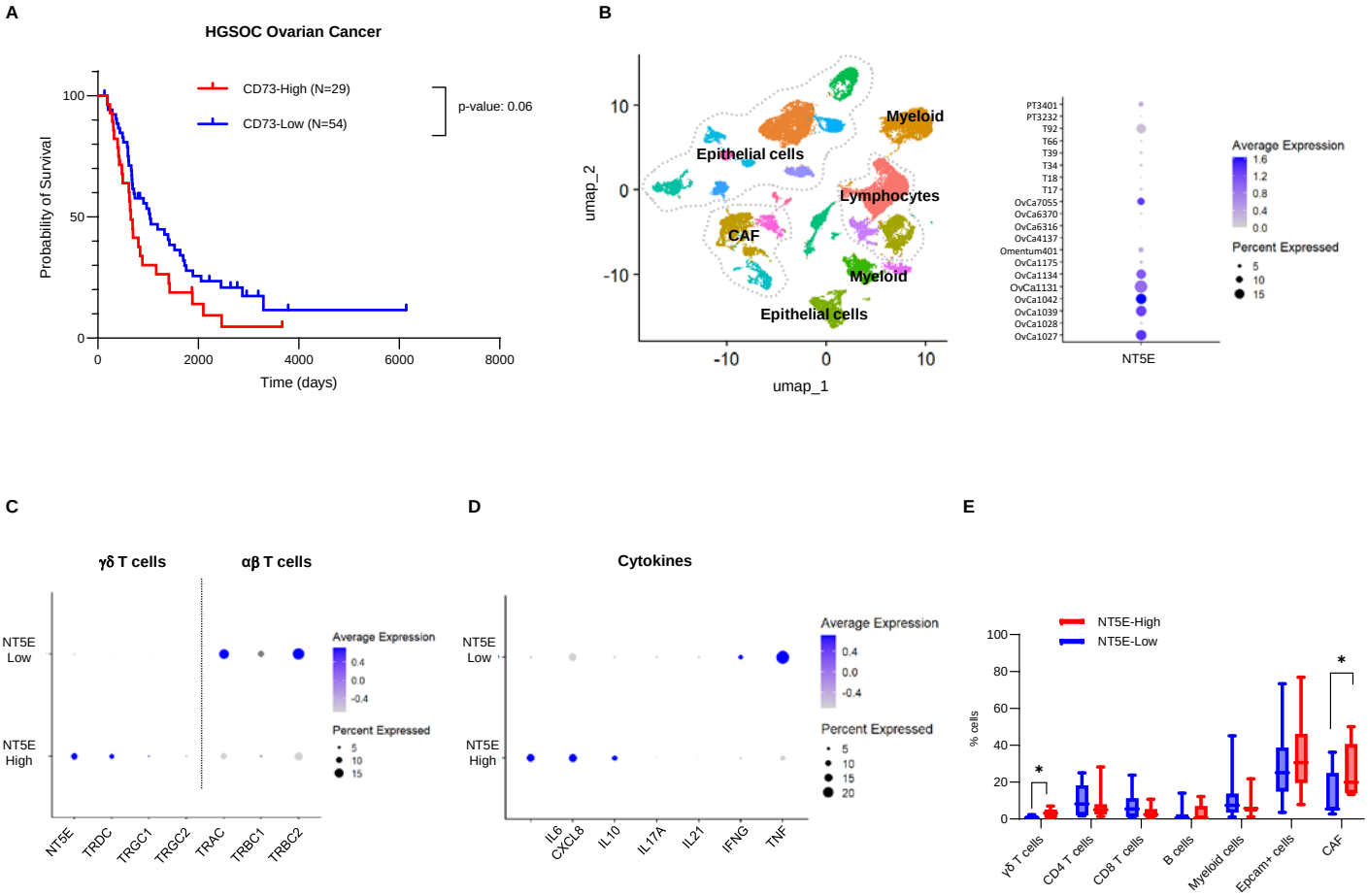

Figure 2. Analysis of single-cell RNA sequencing data from 20 naive HGSOC patients

(A) Kaplan-Meier survival plots comparing patient populations with low and high CD73 (NT5E) transcriptomic expression according to the TCGA dataset stratified on the median expression. (B) UMAP plot of single-cell RNA-sequencing data from 20 untreated high-grade serous ovarian cancer (HGSOC) patients, integrating publicly available datasets GSE147082, GSE241221, and GSE235931. Tumor-associated cell populations were identified based on transcriptomic clustering and annotated accordingly. Right panel: Dot plot illustrating the expression of NT5E (CD73) across the 20 patients, aggregated at the whole-tumor level. Dot size indicates the proportion of cells expressing NT5E within each cluster; color intensity reflects the average expression level. (C) Dot plot comparing the expression of T cell receptor (TCR) chain genes between patients with low (NT5E_Low, n = 10) and high (NT5E_High, n = 10) NT5E expression, defined by a median split of average NT5E transcript levels across all patients. Dot size represents the proportion of cells expressing each gene; color intensity indicates the average expression level. (D) Dot plot showing the expression of cytokine genes in the NT5E_low and NT5E_high patient groups, using the same visual scale as in panel C. (E) Bar plot displaying the relative proportions (%) of major cell types within the tumor microenvironment, stratified by NT5E expression group, based on single-cell cluster annotation.

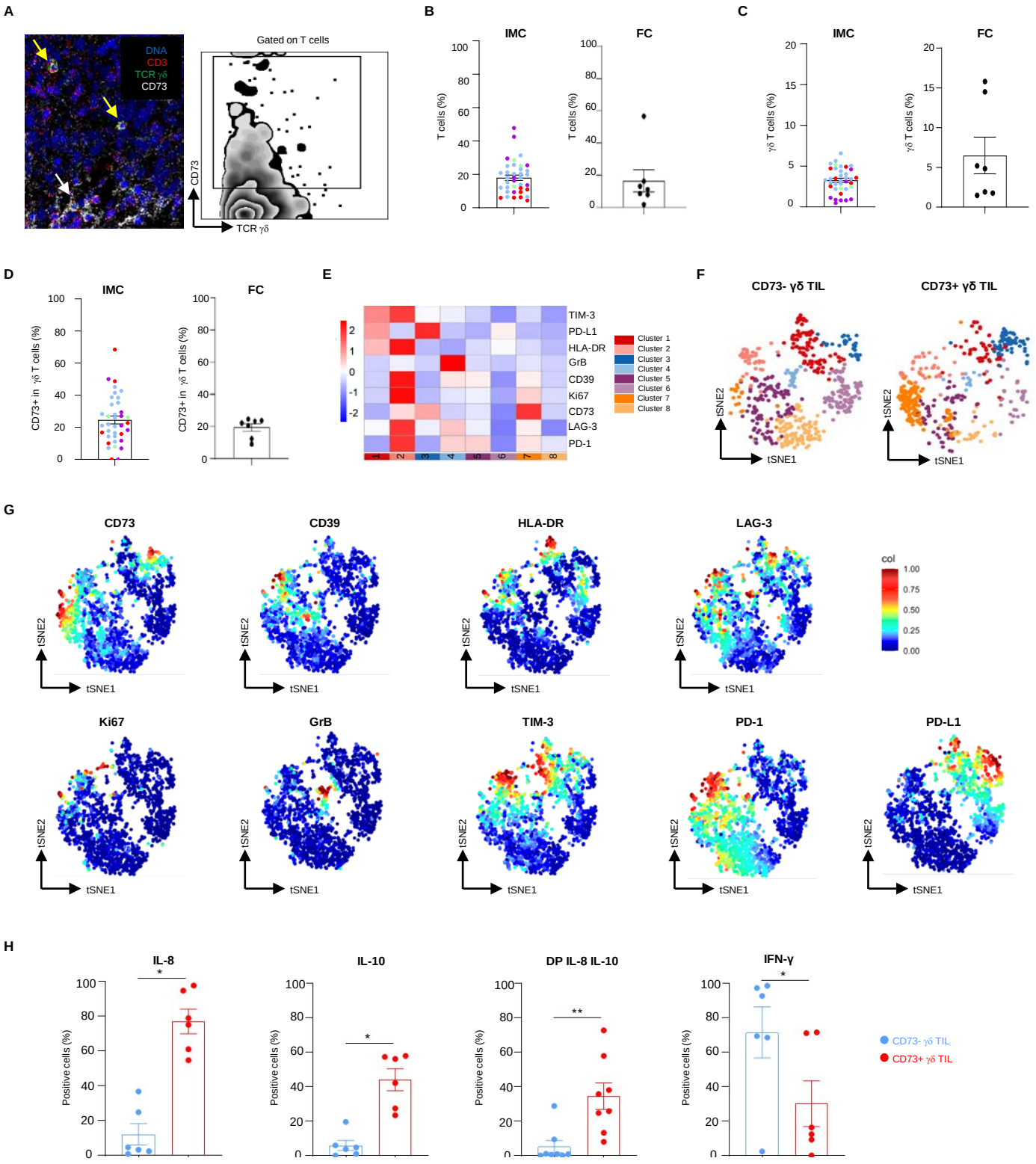

Figure 3. γδ T cell phenotype and function in ovarian cancer tissue

(A) IMC data showing CD73+ and CD73- γδ T cells in an ovarian tumor section (left panel) and the gating (right panel). Dot plots show the percentages of T cells (B), γδ T cells (C), and CD73+ γδ T cells (D) obtained through IMC analysis of 38 ROIs from four patients and flow cytometry analysis of seven patients. For IMC plots, each circle represents a ROI, and each color corresponding to an individual patient. For flow cytometry, each black circle represents an individual patient sample. (E) Heatmap of the mean of signal intensity of each marker and showing the clustering of γδ based on the expression of the listed markers. (F) tSNE plots showing cluster repartition in CD73+ and CD73- γδ T cells. (G) tSNE plots showing the expression of each analyzed marker in the total γδ T cell clusters. (H) Dot plots showing the percentage of CD73+ (red) and CD73- (blue) γδ TILs expressing IL-8, IL-10, double positive IL-8/IL-10 and IFN-γ . Each dot represents an individual patient. Data are the mean ± SEM (n=6); **p < 0.01; *p < 0.05 (Wilcoxon signed-rank test).

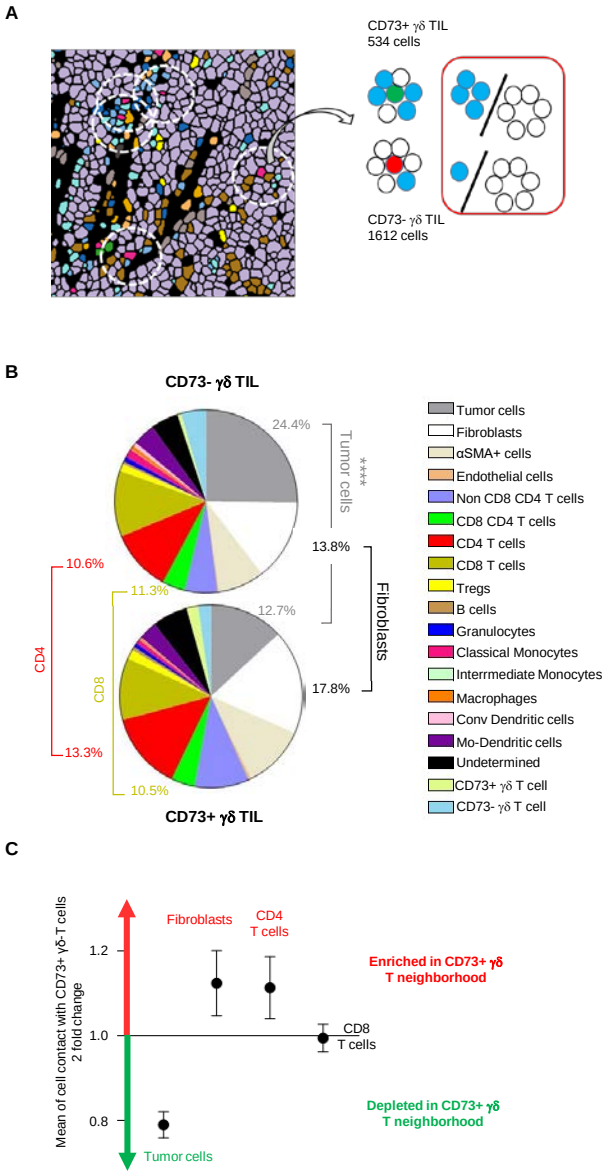

Figure 4. Neighbors of CD73+ and CD73- γδ T cells in ovarian tumor

(A) IMC strategy to extract all neighbors of the CD73+ and CD73- γδ T-cell subsets. (B) Pie charts showing the mean value of each identified cell type in the selected ROIs. Upper panel: Neighbors of CD73- γδ T cells; lower panel: Neighbors of CD73+ γδ T cells. ****p <0.0001 (Wilcoxon signed rank test). (C) The neighborhood cell enrichment represented as the log2 fold change of cell frequency in contact with CD73+ γδ T or CD73- γδ T cells.

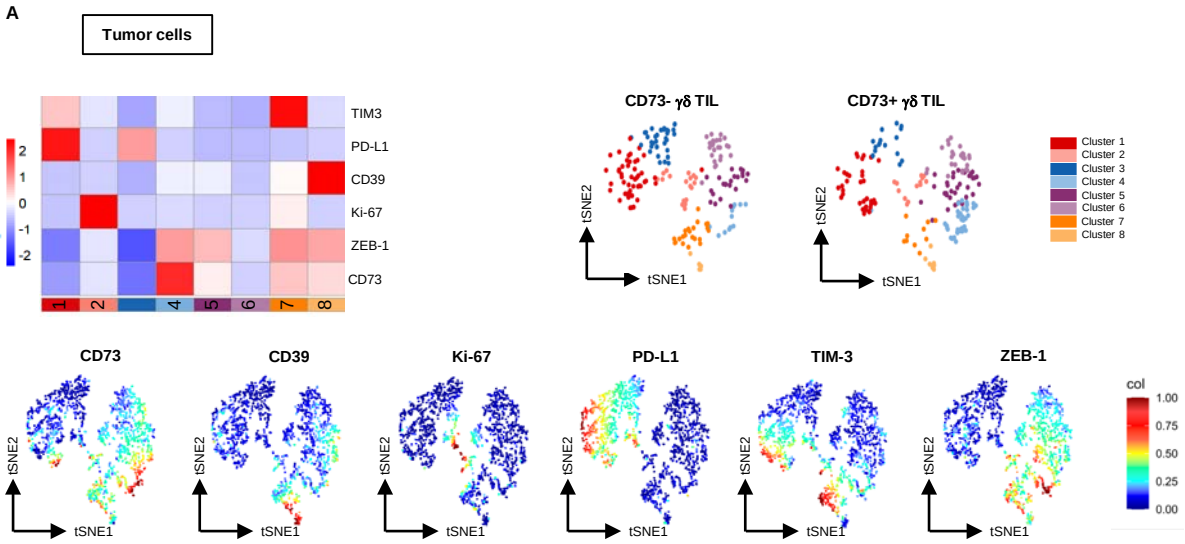

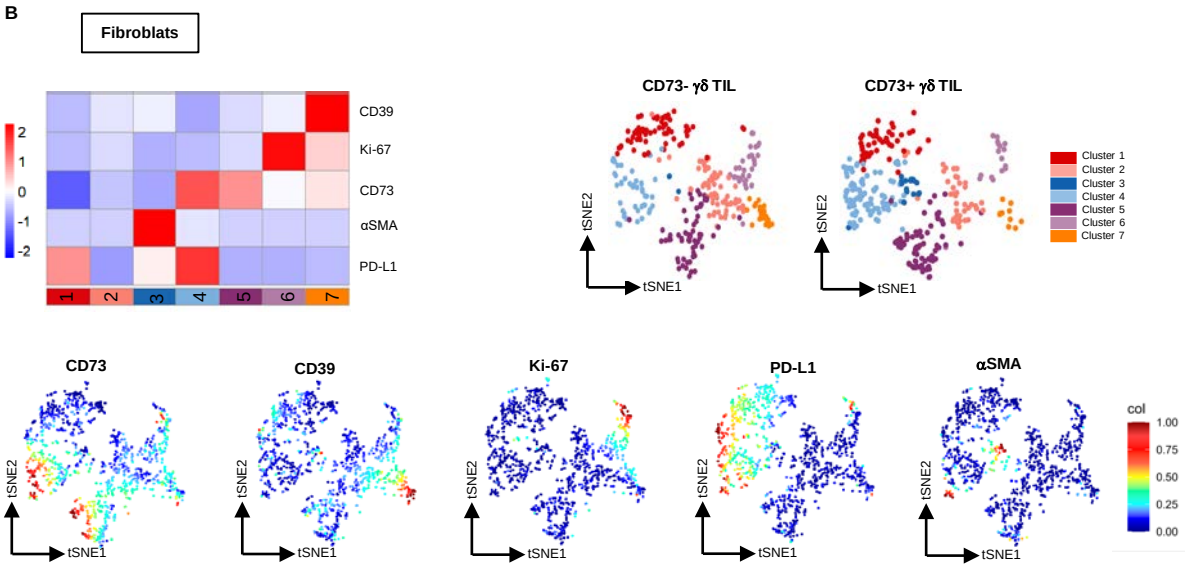

Figure 5. Phenotype of stromal neighbors of CD73+ and CD73- γδ T cell subsets

(A) Heatmap of the mean of signal intensity of each marker and showing the clustering of tumor cells based on the expression of the listed markers (upper left panel) and tSNE plots showing the tumor cell cluster repartition in CD73+ and CD73- γδ T cells (upper right panels). tSNE plot representation of normalized single marker expression in all the sin the total tumor cell clusters (lower panels). (B) Heat map showing the clustering of fibroblasts based on the expression of the listed markers (upper left panel) and tSNE plots showing cluster repartition in CD73+ and CD73- γδ T cells (upper right panels). tSNE plots showing the expression of each analyzed marker in the total tumor cell clusters (lower panel).

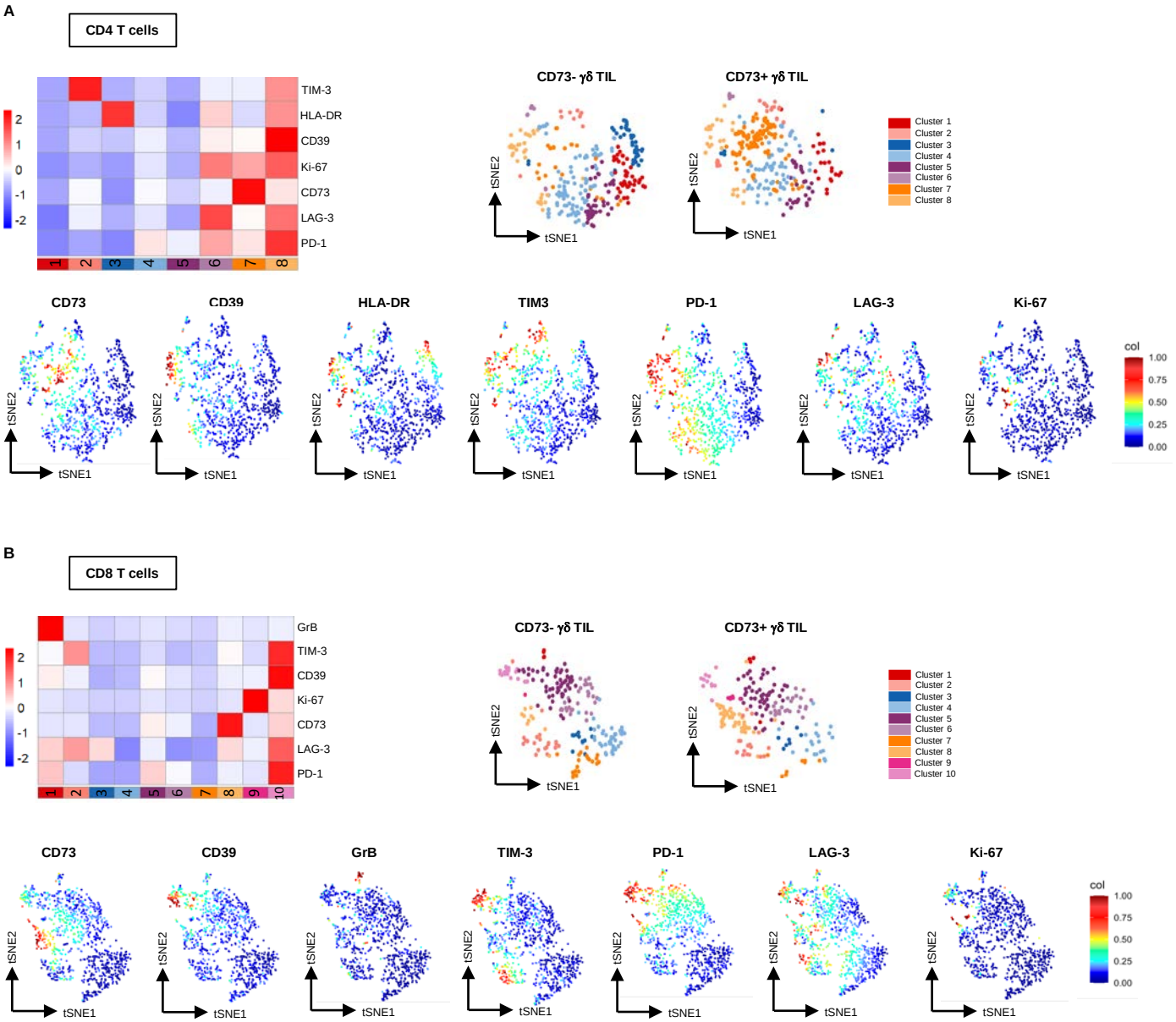

Figure 6. Phenotype of T cell neighbors of CD73+ and CD73- γδ T cell subsets

(A) Heat map showing the clustering of CD4+ T cells based on the expression of the listed markers (upper left panel) and tSNE plots showing cluster repartition in CD73+ and CD73- γδ T cells (upper right panels). tSNE plots showing the expression of each analyzed marker in the total tumor cell clusters (lower panels). (B) Heat map showing the clustering of CD8+ T cells based on the expression of the listed markers (upper left panel) and tSNE plots showing cluster repartition in CD73+ and CD73- γδ T cells (upper right panels). tSNE plots showing the expression of each analyzed marker in the total tumor cell clusters (lower panels).

Trop petit

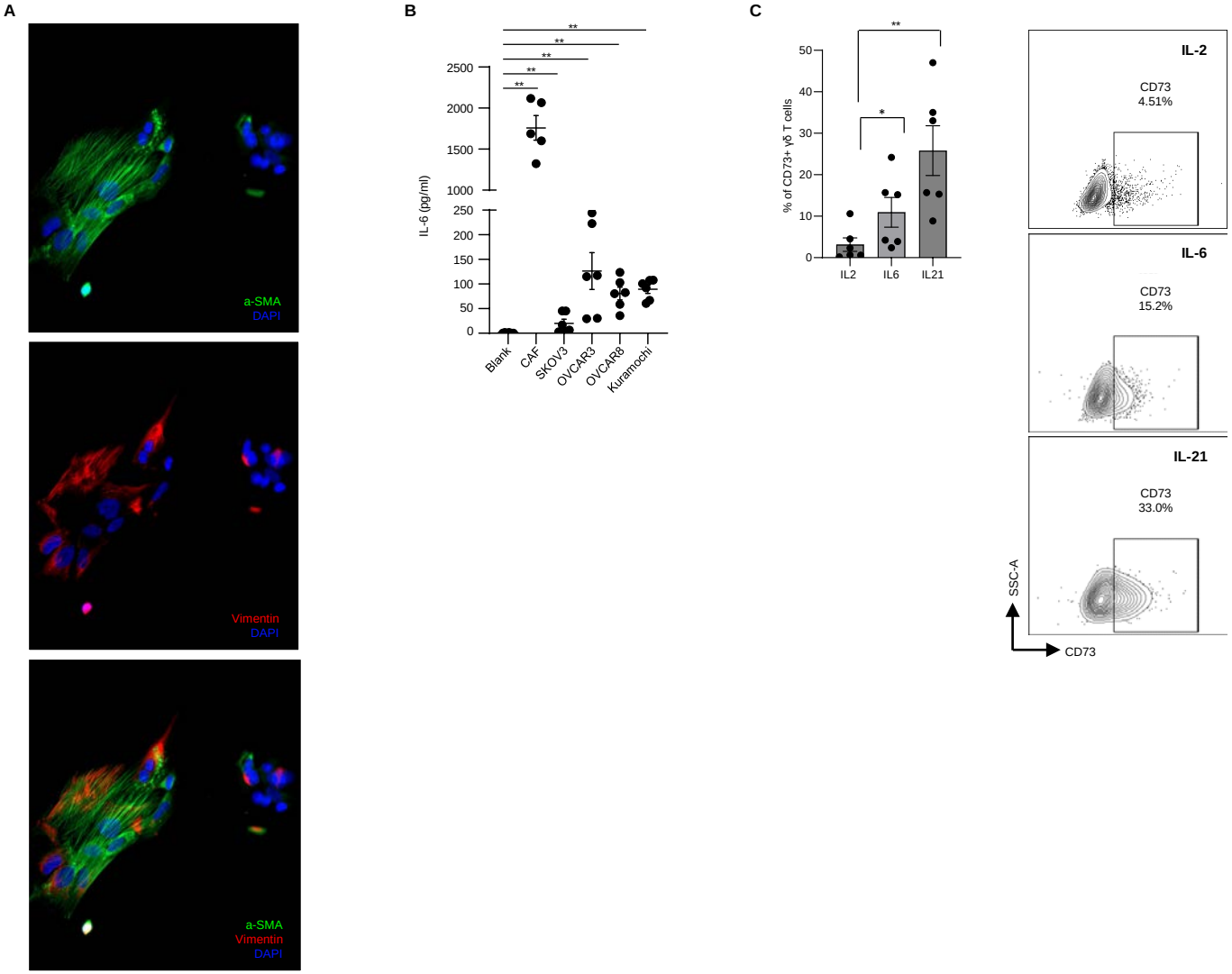

Fig. 7. Impact of IL-6 on CD73 expression by γδ T cells

(A) Immunostaining of CAFs with anti-α-SMA and anti-vimentin antibodies, followed by DAPI. (B) IL-6 production was measured in the supernatants of CAFs and four ovarian cell lines (SKOV3, OVSCAR3, OVCAR8 and Kuramochi). Cells were seeded at 1.10^5 cells/500µl and medium was replaced after 24 hours. Supernatants were harvested after an additional 24 hours and IL-6 was measured by ELISA. (C) After purification, γδ T cells were activated and amplified in the presence of IL-2 alone, and IL-2 with IL-6 or IL-21. CD73 expression was analysed by flow cytometry after seven days. The left panel shows cumulative data from six patients, while the right panel displays a representative dot plot from a single sample. ns: not significant, *: $p<0.05$, ****: $p<0.0001$

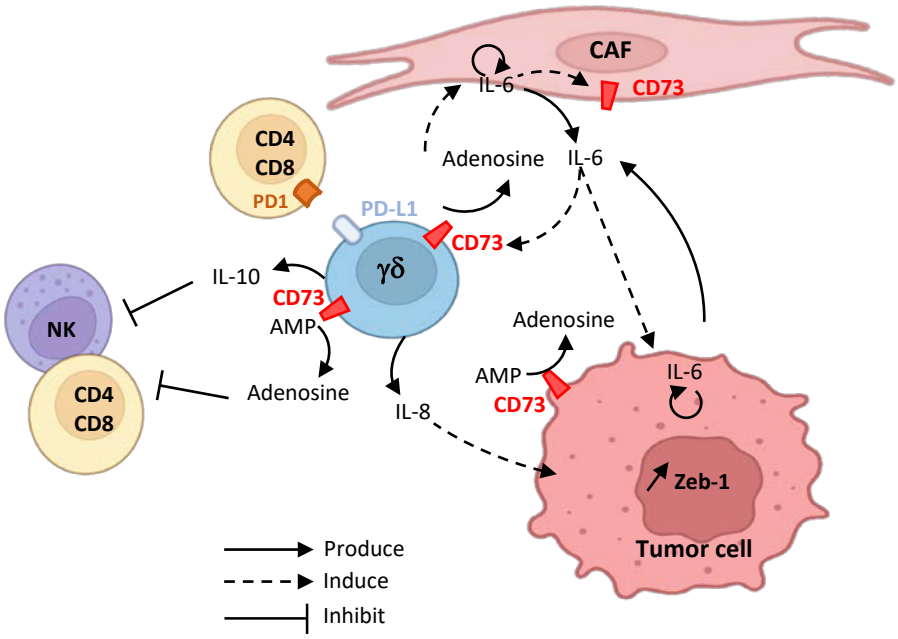

Figure 8. Schematic description of immunosuppressive mechanisms in the neighborhood of CD73+ γδ T cells